THE JOURNAL OF PHYSICAL CHEMISTRY C

Article

pubs.acs.org/JPCC

Interaction of Water Molecule with Au(111) and Au(110) Surfaces under the Influence of an External Electric Field

Ahmed Huzayyin,*[,†,‡] Jin Hyun Chang,[†] Keryn Lian,[§] and Francis Dawson[†]

[†]The Edward S. Rogers Sr. Department of Electrical & Computer Engineering, University of Toronto, Toronto, Canada M5S 3G4

[‡]Electrical Power & Machines Department, Cairo University, Giza, Egypt

[§]Department of Materials Science & Engineering, University of Toronto, Toronto, Canada M5S 3G4

ABSTRACT: The interaction of water monomers with a gold surface is investigated using density functional theory (DFT) to develop a better understanding of the response of a water molecule to an imposed electric field at the surface. Two gold surface orientations, Au(111) and Au(110), are studied. Multiple unique stable adsorption positions of water molecules are identified for each surface orientation, and the results are validated against existing theoretical and experimental data. The values of the adsorption energies do not vary by more than 0.06 eV, which suggests that the potential energy surface of the water molecule interacting with the gold electrode is relatively smooth. The projected density of states and the difference charge density analyses reveal that the interaction mechanism between the water molecule and the gold electrode is a partial exchange of charge rather than a chemical bonding. A normal electric field of magnitude between $\pm 5.0 \times 10^9$ V/m is applied and its effect on the geometry and orientation of the water molecule is analyzed. The change in the geometry of the water molecule in response to the applied electric field shows a strong nonlinearity and asymmetry with respect to the magnitude and direction of the applied field. The interaction between the water monomer and Au electrode with/without the electric field is explained in terms of the interplay of Au−O, Au−OH, and electrostatic interactions. There is a significant difference between the dielectric response of the water molecule on the Au(111) and Au(110) surface that is related to the strength of the adsorption energy of the water monomer to both surfaces.

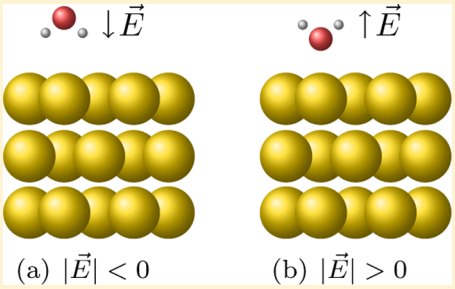

INTRODUCTION

The study of the interaction between the electrode and electrolyte at an interface is of critical importance for many areas of science and engineering, for example, corrosion studies, electrochemical energy storage devices, and electrolyzers. In particular, electrochemical energy storage device modeling faces the challenge of qualitatively and quantitatively identifying the interfacial interaction between the electrode and electrolyte especially during a charging and discharging cycle. It is common to have the electric field, $\vec{E}$, in the electrochemical double layer region in the range of 10^8 to 10^9 V/m[1,2] or even on the order of 10^{10} V/m[3] when an external electric potential is applied across the electrodes. As a consequence, the structure of water (or other ions present in the electrolyte) in this region differs from that of the ultrahigh vacuum environment,[2] which is a common environment for both experiments and density functional theory (DFT) studies.

Water is the main constituent of the electrolyte solution for the majority of applications, and as a result, the interface between the water and electrode has been the main subject of study in the past. There are two competing interactions that are involved in shaping the dynamics of the water−electrode interface: water−water interactions (via hydrogen bond) and water−electrode interactions.[4] The overall structure and dynamics of the interface region is a result of the complex interplay between these two competing interactions.[4] This interplay is significant for most of the transition metal electrodes where the energies of the water−water and water−metal interactions are in the same order of magnitude.[5] This poses an extra challenge to both experimental and computational investigations.

The focus of this work is on the interaction between a water monomer and the electrode in the presence of an external electric field. Having one water molecule at the interface eliminates the water−water interaction, and the response of the water−metal interaction to the electric field is characterized. The interface with more than one water molecule is expected to respond differently to the applied electric field due to the presence of the water−water interaction. However, the characterization of the response of the water−metal interaction to the electric field is an important milestone for the future investigation of the interface involving a number of water molecules. The present work is an essential first step toward a better understanding of the polarization of the water double layer next to the electrode's surface, which is a phenomenon of a major importance in electrochemical energy storage devices. In the case of a double layer, a new balance between water−water and water−metal interactions is achieved under the

Received: August 9, 2013
Revised: January 22, 2014
Published: January 23, 2014

   dx.doi.org/10.1021/jp408001t | *J. Phys. Chem. C* 2014, 118, 3459−3470

influence of the applied electric field. The present work investigates a gold electrode with a clean surface free of any defects.

In recent years, there have been considerable efforts on both computational and experimental fronts to include the impact of the electric field. On the computational side, a number of methods have been used to self-consistently create an interfacial electric field in a DFT framework. The methods include imposing a net charge on the system,[6−8] adding an atom/ion that donates (accepts) a net charge to (from) the electrode,[9] creating a constant electric field across the system.[10−14] The electric field in the first two methods is created by the localized charge in the system (i.e., near the surface of the electrode), whereas a constant electric field is created by two sheets of uniform charges along the boundary faces of the unit cell in the last method. The last method (constant electric field) is used for this work with the direction of the electric field oriented normal to the electrode surface with a maximum magnitude of 5×10^9 V/m. The electric field is correlated to the surface charge density. The maximum electric field magnitude of 5×10^9 V/m corresponds to a surface charge density of ± 4.43 μC/cm^2.

There are a number of experimental methods that are widely used for the purpose of understanding the interaction of water with various types of metals. Low-energy electron diffraction (LEED) experiments have been carried out to study the interaction of water with various surfaces of Pt, Ru, and Au.[15−17] The interaction of perchloric and sulfuric acid with Au(111) was studied[18−20] using surface-enhanced infrared absorption spectroscopy combined with an attenuated-total-reflection technique (ATR-SEIRAS).[21] Isolated water clusters can now be studied using scanning tunnelling microscopy (STM), as was demonstrated for the case of Pt, Ag, and Cu.[22−25] These methods allow one to vary the magnitude of an external electric field (or the bias voltage of the electrode) and measure the orientations of water molecules on the surface. However, it remains challenging to measure the interaction between the water monomer and electrode.[26,27]

There are several notable review articles that provide a background and recent progress on the topics that are relevant to this work. Thiel and Madey[27] provided a comprehensive overview of the water molecule and associative/dissociate adsorption of water molecule(s) on various types of electrodes and electrode surfaces. Hodgson and Haq[4] discussed the water adsorption and cluster formation on a metal surface which in turn lead to monolayer and multilayer formation. More recently, Carrasco et al.[28] summarized the progress made after 2009 on the molecular picture of the interaction between the water and metal electrodes and the status of the field as of 2012. Lastly, Stuve[3] summarized the effect of the electric field on the ionization of water on the basis of computational and experimental results and suggested how experimental methods could be used in future to make measurements in the presence of high electric fields.

A substantial improvement of our understanding of the water−electrode interface has been made in recent years as a result of both computational and experimental efforts. One example of an improvement is both experimental and theoretical evidence to challenge the common assumption of the general validity of the water bilayer model.[28] In spite of these developments, the details of water monomer adsorption on metal surfaces and the overall dynamics of the interface is still not well understood,[29,30] particularly under the influence of the external electric field.

METHODOLOGY

Density functional theory (DFT) is the most widely used computational quantum mechanics method applied on the scale of hundreds of atoms because it demands less computing resources than other methods. Using DFT and optimization (relaxation) of nuclear positions within the framework of the Born−Oppenheimer approximation the minimum energy structure (ground state) can be determined for a system of electrons and nuclei. DFT determines the eigenvalues (energy states) and their corresponding eigenfunctions (wave functions) from which various features of matter can be obtained from first principles. DFT can determine atomic structures within 3% of experimental measurements and relative energies (e.g., formation energy and adsorption energy) within 10−20% of experimental measurements.[31] DFT can provide the density of states (DOS) and charge density for the ground state atomic structure. In addition, the partial density of states (PDOS) analysis can explain the nature of the interaction between the atoms by determining the contribution of each orbital of each atom in the system to any given state. DFT also allows one to study the effect of an applied electric field.

Computations were carried out using the SIESTA code.[32] In the present work, the interaction of the nuclei and core electrons with the valence electrons was approximated using Troullier−Martin pseudopotentials.[33] The wave functions were expanded using a double-ζ plus polarization basis set (DZP). The exchange−correlation functional was approximated using the generalized gradient approximation (GGA) with the Perdew−Burke−Ernzerhof (PBE) flavor.[34] Optimization of atomic nuclei positions was done using the conjugate gradient (CG) method by requiring the force on each atom to be less than 0.05 eV/Å. The force was determined within the SIESTA code according to the Hellman−Feynman theorem,[35] including the Pulay correction.[36] The mesh cutoff was 250 Ry (∼3400 eV). The computational parameters such as the mesh cutoff, k-points, and basis sets, were chosen to ensure that the energy converges within 0.01 eV.

The work was carried out using periodic boundary conditions. A supercell of a gold slab with two water molecules on the surfaces at each side was used to maintain symmetry. Enough vacuum was included in the unit cell to ensure that no dipole−dipole interaction existed between neighboring images created by the periodic boundary conditions. The size of the slab was chosen such that the bulk properties and its periodicity were reproduced in the center of the slab. The recovery of the periodicity was determined through the planar average potential. The Au(111) and Au(110) slabs consist of 9 and 13 layers, respectively. The size of the supercell surface is $2\sqrt{3} \times 3$ for Au(111) and 3×4 for Au(110). The size of the supercell surface for Au(111) and Au(110) was chosen to ensure no interaction of the water molecule with its periodic images created by the periodic boundary conditions. All the atoms of the slab were allowed to relax and the ground state structure of the slabs is determined accordingly. The work function for the slab was computed using the "bulk plus band line up" method.[37] The Au(111) surface used corresponds to the unreconstructed surface. The more stable "herringbone" reconstructed Au(111) surface will be included in future work. Vibrational frequency analysis was used to inspect the stability of adsorption sites. Vibrational frequencies were computed using a finite difference scheme with an atomic displacement of 0.01 bohr. Due to constraints on computational resources, only the atoms of the water molecule and the first three gold layers in the slab were allowed to vibrate whereas the gold atoms of the fourth layer were fixed. This approximation yields the same frequencies as when more layers were included in the analysis. The Vibra postprocessing tool (included with the SIESTA 3.1 release) was

dx.doi.org/10.1021/jp408001t | J. Phys. Chem. C 2014, 118, 3459−3470

used for the vibrational frequencies analysis. The models and methods used in the present work have been validated by comparing the physical parameters of the gold electrode and (isolated) water monomer to the experimental data. Work functions of Au(111) and Au(110), Φ, the lattice constant of gold electrode in bulk, a_0, bond dissociation energy of the water monomer, $D^{O}_{H_2O}$, bond length, d_{O-H}, and bond angle, ∠H−O−H, of the water monomer are compared to the experimental values, as shown in Table 1. For an isolated water molecule, the

Table 1. Physical Parameters of Isolated Water and Gold Electrode and Their Values

physical parameter	this work	experimental	% error
d_{O-H} (Å)	0.9804	0.9572[39]	2.4
∠H−O−H (deg)	103.63	104.52[39]	0.89[a]
$D^{O}_{H_2O}$ (eV)	3.02	2.85[40]	5.8
a_0 (Å)	4.23	4.08[41]	3.7
(111) Φ (eV)	4.94	5.26[42]	6.1
(110) Φ (eV)	4.89	5.20[42]	6.0

[a]in degrees.

symmetric stretch (ν_1), antisymmetric stretch (ν_2), and symmetric bend vibrational mode (ν_3) were computed as 3684, 1579, and 3811 cm^{-1}, respectively, with respective errors of 0.5%, 1.0%, and 1.4% compared to the Ne matrix experimental values in ref 38. No correction factors were used in the present work. The DFT determined values are in acceptable agreement with experimental values.

The water molecule was allowed to relax on the surface of the gold slab to determine its stable positions/orientations in the absence of an electric field. The water molecule was also allowed to relax in the presence of the electric field as a part of a separate study to analyze the polarization of the water molecule on the surface.

RESULTS AND DISCUSSION

Stable Sites of Water Molecule. Prior to investigating the impact of the external electric field, stable sites of water monomer were identified on Au(111) and Au(110) via the structure optimization computations in the absence of the external electric field. This is also referred to as a point of zero charge (pzc). Four stable sites were identified for each surface orientation, which are shown in Figure 1. The names of the stable sites, adsorption energies, E_{ads}, of the stable sites, and binding angle, α, are shown in Table 2. The sites are numbered in increasing order from left to right in Figure 1. Adsorption energy is defined such that negative adsorption energy corresponds to exothermic adsorption. The binding angle of the water molecule is defined as an angle between the tangential plane of the electrode and a vector from the oxygen atom to the center of two hydrogen atoms as shown in Figure 2. With this definition, 0° corresponds to the orientation where the water molecule is parallel to the surface, and positive and negative angles represent the orientations toward "hydrogen up" and "hydrogen down" configurations, respectively.

Multiple stable adsorption sites are identified as shown in Figure 1 and Table 2. However, one cannot exclude the presence of other stable sites. The results show the general trends that a smaller separation distance between the water molecule and the closest Au atom (d_{O-Au}) and a more parallel orientation of the water to the surface (i.e., α closer to 0°) correspond to a

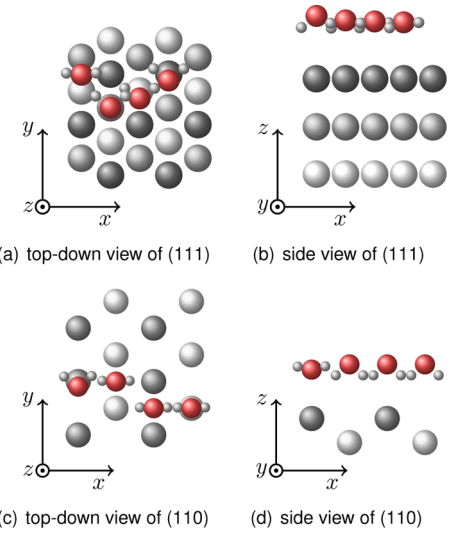

Figure 1. Stable sites of water monomers on Au(111) and Au(110) without an external electric field. Gold atoms are displayed in varying shade levels to distinguish the layers.

Table 2. Adsorption Energy and Binding Angle of Water Monomer at Stable Sites

	name		E_{ads} (eV)[a]		α (deg)[b]	
position	(111)	(110)	(111)	(110)	(111)	(110)
1	bridge	atop	−0.09	−0.19	−81.8	17.3
2	hcp hollow	long bridge	−0.12	−0.13	−13.6	−85.9
3	fcc hollow	short bridge	−0.13	−0.14	−31.4	−85.8
4	atop	hollow	−0.15	−0.14	−1.5	−85.9

[a]$E_{ads} = E_{H_2O/Au} - E_{H_2O} - E_{Au}$, where $E_{H_2O/Au}$, E_{H_2O}, and E_{Au} are the total energies of the system with water and gold electrode, isolated water monomer, and the gold electrode without the water monomer, respectively.; [b]An angle from which the water molecule is oriented parallel to the electrode surface. Positive represents the "hydrogen up" configuration.

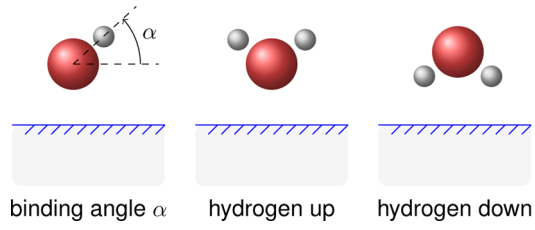

Figure 2. Binding angle of water monomer, hydrogen up and down configurations.

higher adsorption energy. The atop sites, where the water molecule is close to being parallel to the surface, are the most stable adsorption sites for both Au(111) and Au(110). The variation in the distance between the oxygen atom and the gold surfaces Au(111) and Au(110) are found to be relatively small for all stable positions, and the distances are between 2.90 and 3.23 Å for Au(111) and between 2.74 and 3.04 Å for Au(110).

Adsorption Energies at Stable Sites. The adsorption energies for stable sites were in the sequence atop > fcc hollow > hcp hollow > bridge for Au(111) and atop > hollow ∼ short bridge > long bridge for Au(110). Aside from the atop position, other stable sites of the water monomer on Au(111) are rarely discussed. In the present work, multiple stable sites and adsorption geometries other than the nearly flat atop site have

dx.doi.org/10.1021/jp408001t | J. Phys. Chem. C 2014, 118, 3459−3470

been identified. This is in general agreement with the recent work in ref 43 where PBE and optB88-vdW (van der Waals interactions included) functionals have been used to determine six adsorption orientations ("S1 to S6") of the water monomer on Au(111). Five of these orientations are similar to those at the four positions identified in the present work. The two flat molecules on the atop positions "S1 and S2" are most stable (as in position 4 in the present work). The S3 is similar to position 2 (hydrogen down by 13°) in the present work and S5 is similar to position 3 (hydrogen down by 31°), S6 is similar to position 1 (hydrogen down by 82°). The angles were not mentioned explicitly in ref 43 so only qualitative comparisons are made with the figures in ref 43. In addition, using PBE, four stable adsorption sites of a water monomer on Cu(110) on atop, bridge, and hollow sites have been identified proving earlier experimental speculations about the presence of stable sites other than the atop sites.[44]

Au(110) on average displayed higher adsorption energy than Au(111), which confirms that the atomically open surface orientation in general exhibits higher adsorption energy than a more closed orientation.[13] A common conclusion from the previous DFT[5,26,45] and experimental investigations[18−20] is that the atop site is the most favorable site for the water monomer on the FCC(111) surface with near parallel orientation. The result of this work shows that the atop site has the highest adsorption energy, which is in agreement with the literature. The atop site on Au(110) also exhibits the highest adsorption energy and is also the most stable site on Au(110), which is consistent with the STM and DFT study for Cu(110).[46] The fact that the atop site is most favorable on both surfaces is in agreement with ref 27.

Although the atop site is energetically most favorable, the difference in energy with the second most stable sites is small. Furthermore, the maximum variation in the adsorption energy at four stable sites of Au(111) and Au(110) were both around 0.06 eV. The small variation suggests that the potential energy surface (PES) of water adsorbed on the gold surface is smooth. On the basis of the small variation in adsorption energies, thermal vibration may trigger the water monomer to move along the surface at room temperature where the thermal energy is approximately 0.03 eV. This is also supported by the finding from the STM measurements that a water molecule is mobile on Au(111) and Au(110).[47] Thus, it is likely that at low coverage, water molecules can be present at sites other than the atop site. The range of adsorption energies of −0.09 to −0.19 eV for all stable positions on Au(111) and Au(110) suggests that the nature of binding is weak chemisorption/physisorption, again in agreement with previous conclusions.[5,27,48] Further investigation is required to determine the energy barrier between stable sites to make an accurate remark about the relative stability of the identified sites. Although the nudged elastic band method is needed to determine the energy barriers, one can determine whether the converged state is translational or stable by investigating the vibrational frequency spectrum. The presence of negative frequencies in the spectrum indicate that a state is at a transitional position on the PES.[49] Applying such a criterion suggests that only position 3 on a Au(110) surface is a transitional state.

Experimental estimates of adsorption energies of water on gold are provided by Heras et al.[50] and Wells et al.[48] where the ranges are between 0.13 and 0.40 eV and between 0.13 and 0.39 eV, respectively. Such a wide range is attributed to the variation in the surface coverage of water where the higher surface coverage increases the experimentally measured adsorption energy.[48] Because our computation is designed to replicate the lower limit of surface coverage (e.g., the apparent surface coverage on Au(111) and Au(110) are both 1/12 monolayer (ML)) where there are minimal water−water interactions, the lower limit of 0.13 eV is used and is within the range of computed values.

Further discussions are focused on the water monomer located at the atop site of Au(111) and Au(110), which is the most stable adsorption site. Other sites are also investigated and similar trends and qualitative conclusions were drawn.

Adsorption Geometry of Water Molecules. The structure of an adsorbed water monomer on the atop site of Au(111) is used for main comparison with the literature due to the abundance of data on its structure based on DFT computations.[5,26,45,51−53] To the best of the authors' knowledge, the only DFT work in the literature on the water structure at other sites of Au(111) is in ref 43 and on monomeric water adsorption on Au(110) is in ref 44. The values of structural parameters from this work and the reviewed literature are shown in Table 3. There is good agreement in both bond angle and bond length of the water molecule; the maximum difference in bond angle and bond length between this work and others are 1° and 0.01 Å, respectively. A minor discrepancy is found in other parameters such as E_{ads} and d_{O-Au}, where the maximum difference is 0.04 eV and 0.29 Å, respectively. The differences are not considered significant especially for the given level of variation in both experimental and theoretical results.[5,26] The most notable differences are for the lateral displacement from the exact atop site, ΔO_{xy}, and the binding angle, α. The differences might be related to the various sizes of the surface of the supercell or the number of layers forming the slab. The work by Nadler and Sanz[52] and the present work employ the largest supercell (7 layers with 16 Au atoms in each layer for ref 52 and 9 layers with 12 Au atoms in each layer for this work) and they exhibit the best overall agreement in results with one another.

Table 3. Structure of Water Monomer Adsorbed on Atop Site of the Au(111) Surface

source	E_{ads} (eV)	d_{O-Au} [a] (Å)	d_{O-H} (Å)	ΔO_{xy} [b] (Å)	∠H−O−H (deg)	α (deg)
this work[c]	−0.15	2.92	0.98	0.33	103.8	−1.5
refs 5 and 26[d]	−0.13	3.02	0.97	0.06	105	13
ref 45[e]	−0.14	2.63	0.98	0.06	105	10
ref 53[f]	−0.11	2.67	0.98		105	6
ref 52[g]	−0.11	2.79		0.40		−0.8
ref 51[h]	−0.12	2.8				5
ref 54[i]	−0.17					flat

[a]Distance between the oxygen atom of water and the underlying gold surface atom. [b]Lateral displacement of exact atop site where oxygen atom vertically aligns with underlying gold atom. [c]1/12 ML, 9 layers. [d]1/4 ML, 5 or 6 layers. [e]1/9 ML, 3 layers. [f]1/9 ML, 7 layers. [g]1/16 ML, 7 layers. [h]1/12 ML, 4 layers. [i]1/4 ML, 3 layers.

There is a correlation between the structural details of the adsorbed water molecule and the size of the supercell surface. Michaelides et al.[5] noted that the difference in energy is between 0.03 and 0.05 eV when the size of the supercell surface is varied from 2 × 2 to 3 × 3 without any reference to the structural change, whereas Phatak et al.[45] argued that a 2 × 2 cell is small enough to include the unphysical water−water interaction between the periodic images. Nadler and Sanz[52]

dx.doi.org/10.1021/jp408001t | J. Phys. Chem. C 2014, 118, 3459−3470

performed the comparison for a supercell surface size from 2 × 2 to 4 × 4 and the results show a fluctuation in α and ΔO_{xy} between −5.6 and +3.8° and 0.15 and 0.40 Å, respectively. They noted that the adsorption geometry of the water monomer is sensitive to the change in the supercell surface size while the adsorption energy remained insensitive.[52,55] Nadler and Sanz[52] also studied the influence of the number of layers in a slab by varying it from 4 to 8 and showed that both α and ΔO_{xy} fluctuate between −0.8 and +8.3° and 0.13 and 0.40 Å, respectively. Such dependency of α and ΔO_{xy} on the size of the supercell (i.e., both surface size and the number of layers) is observed in Table 3, and it supports the previously mentioned agreement between the adsorbed water structure in the present work and ref 52. The differences in the structure of the adsorbed water molecule and the adsorption energy do not contribute to the qualitative conclusions drawn from the computation results of the present work. For a water monomer adsorbed with a flat orientation at the atop position of Au(110), the d_{O-Au} and E_{ads} were 2.59 Å and 0.21 eV, respectively, in ref 44, compared to 2.74 Å and 0.19 eV in the present work. The structure and E_{ads} of the water monomer at the atop site of Au(111) of the present work agrees well with the trend pointed out in ref 56 for other transition metal surfaces as shown in Table 4. The trend shows that E_{ads}, ∠H−O−H, and α decrease

Table 4. Adsorption Energy and Structure of Water Monomer Adsorbed on Atop Site of Transition Metal Surfaces

	E_{ads} (eV)	d_{O-M}[a] (Å)	d_{O-H} (Å)	∠H−O−H (deg)	α (deg)
Ru(0001)[b]	−0.42	2.31	0.99	105.3	11.5
Rh(111)[b]	−0.36	2.34	0.99	104.6	4.2
Pd(111)[b]	−0.27	2.33	0.98	104.8	5.1
Ag(111)[b]	−0.15	2.67	0.98	104.2	0.5
Au(111)[c]	−0.15	2.92	0.98	103.8	−1.5

[a]Distance between the oxygen atom of water and the underlying metal surface atom. [b]Values taken from ref 56. [c]This work.

while d_{O-M} increases as the atomic weight of the transition metal increases.

The result of the present work agrees well with the experimental results[2,18−20] where the water molecules lie parallel to the Au(111) surface at the pzc. Furthermore, on the basis of experimental results, Garcia-Araez et al.[30] suggested a slight negative α for the water molecule on a Au(111) surface for potentials $0 < E < 0.5$ V. The results of the present work and ref 52 exhibit the most parallel orientations among the surveyed literature (with a slightly negative α), which may be attributed to the large size of the supercell. It should be pointed out that it is challenging to measure the true water monomer−metal interaction due to the cluster formation in the experimental settings even at the low surface coverage conditions[26,27] and thus, meticulous comparison between the experimental and computational results should be done cautiously. The fact that the two most stable sites of the water monomer found on Au(111) have a nearly flat orientation to the surface is in qualitative agreement with the experimental results. A good numerical agreement with other computational results and a qualitative agreement with the experimental results suggest that the reported structures are indeed valid.

The van der Waals (vdW) interactions are not included in the present work. The vdW interactions have been demonstrated, in ref 43, to increase the absolute value of the E_{ads}. However, it was concluded that "the relative stability, adsorption sites, and adsorption geometries of competing water adsorption structures rarely differ when comparing results obtained with semi-local functionals and the non-local vdW density functionals, which explains the previous success of semi-local functionals in characterizing adsorbed water structures on a number of metal surfaces."[43] It is also noted that "although vdW enhances the bonding with the substrate, the water−water interaction energies within the clusters remains largely unaffected by the inclusion of vdW dispersion forces. In addition the geometries of the water monomers and clusters on the various surfaces are not affected to any great extent by the inclusion of vdW dispersion forces, which explains the previous success of GGA functionals in predicting adsorption structures of water on metals."[43] It is worth noting that some of the sites identified as stable with the inclusion of vdW forces were rendered unstable using PBE.[43] This might be attributed to the fact that the PES is smooth and the relatively small vdW interactions can be influential. Nevertheless, five of the six stable sites have geometries similar to those of the four positions identified in the present work. In addition, the d_{O-Au} values in ref 43 of 3.084, 2.853, and 2.750 Å using various vdW functions agree well with the 2.92 Å of the present work. The present work shows that higher adsorption energy implies that higher external field is needed to achieve a complete rotation of the molecule. The magnitude of such field might be affected by the inclusion of vdW. The inclusion of the vdW when the effect of the external field is studied is an important aspect that will be the topic of future investigations.

Nature of H_2O−Au Interaction. The interaction of the water monomer with the gold surface in the absence of an external field is governed by three factors: (1) the interaction between the oxygen atom and the gold atoms (Au−O), (2) the interaction between the OH group with the gold atoms (Au−OH), and (3) the interaction between the water dipole and the surface (Au−dipole), which can also be explained in terms of the self-interaction of the dipole and its image mandated by the method of images. As shown in Figure 1, there is a variation in the water orientation depending on its location above the electrode. A notable tendency, however, is that water molecules tend to lie virtually parallel to the electrode on atop sites but they lie almost perpendicular to the electrode with hydrogen down on bridge sites. The hollow sites exhibit a mixed behavior where the water molecule lies almost perpendicular to the electrode on Au(110) but in a tilted orientation on hcp and fcc hollow sites on Au(111).

A difference charge density, $\Delta\rho$, analysis of H_2O and H_3O next to Au(111) was conducted to further understand the nature of the interaction between the water molecule and the gold electrode. The results show that the interaction between the surface and H_2O involves only a partial charge transfer between the H_2O and the surface whereas a whole electron transfer takes place in the case of H_3O as shown in Figure 3. This indicates that the nature of the interaction between the water monomer and gold surface is based on the Au−O and Au−OH covalent interactions.[5] The charge accumulation and depletion trends shown in Figure 3 for the water molecule agrees with the reported electronic reactivity function (Wilke function) based analysis[56] as well as the difference charge density analysis[56,57] for other 4d metals including Ag and Pt which are expected to behave qualitatively similar to Au.

dx.doi.org/10.1021/jp408001t | J. Phys. Chem. C 2014, 118, 3459−3470

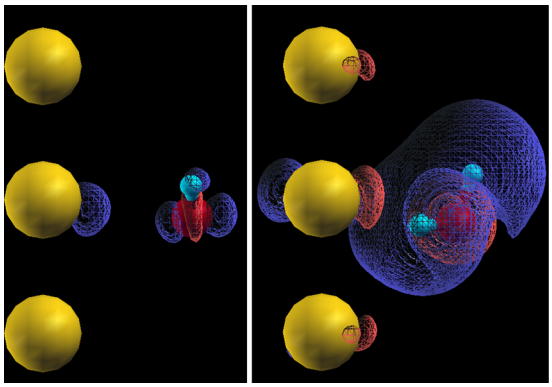

Figure 3. Difference electron charge density for Au(111)−H_2O (left) and Au(111)−H_3O (right) with isosurfaces corresponding to regions of charge depletion (blue) and accumulation (red). Same charge density value is used for isosurfaces for a direct comparison.

The nature of the interaction of the water molecule at each site cannot be strictly attributed to only one of the Au−O, Au−OH, or Au−dipole interactions. However, comparing the PDOS and bond lengths of the water molecule on the Au surface to those of an isolated water molecule clearly indicates which type of interaction is dominant at a specific adsorption site. An elongation of the water bond length, d_{O-H}, was observed for the water monomers at all of the stable sites. The maximum elongation of 1% occurs at bridge sites of Au(111) and Au(110). Among the bridge sites of Au(110), elongation was slightly greater at the long bridge site than the short bridge site. This elongation indicates the presence of an Au−OH interaction. A higher degree of elongation on bridge sites suggests a stronger Au−OH interaction. Atop sites, on the other hand, exhibit stronger Au−O interaction with less Au−OH interaction indicated by smaller elongation of d_{O-H} and higher adsorption energy. Furthermore, the results show a correlation between the molecule geometry and the dominance of one interaction over the other, with the two extremes being the flat orientation where the Au−O interaction is dominant and the perpendicular hydrogen down orientation where the Au−OH interaction is dominant. This is further supported by PDOS analysis.

The PDOS analysis suggests, as noted previously by other authors,[26,27] that the $1b_1$ orbital (water "lone pair" orbital) and $3a_1$ orbital are the most important orbitals. These are the orbitals that contribute the most to the H_2O/Au interaction, with the $1b_1$ being the most dominant at the atop site. The dominance of the $1b_1$ orbital suggests that the Au−O interaction via oxygen lone pairs is stronger than the Au−OH interaction. The dominance of lone pair interaction is also reported elsewhere.[10,29,53,58] However, the PDOS analysis on bridge and hollow sites shows that the main interaction comes from the OH group (attributed to $3a_1$). Although the water monomer adsorbed on the gold surface is usually explained in terms of the lone pairs ($1b_1$), the PDOS analysis in Figure 4 shows that the $3a_1$ orbital plays a major role in such an interaction particularly as α becomes more negative. As α becomes more negative, the state corresponding to the $3a_1$ orbital from both the oxygen atom and hydrogen atoms becomes further distorted and broadened compared to the isolated molecule case thus indicating the $3a_1$ (Au−OH) participation in the adsorption process to the metal surface. The flatter the adsorption angle the more similar the $3a_1$ orbitals are to the isolated atoms. On the other hand, the state corresponding to the lone pair orbital becomes distorted and broadened, which is in agreement with previous work.[56] The PDOS analysis for Au(110) demonstrates a similar trend and correlation with α.

The interaction of the water dipole with the surface would mandate that the water molecule sits perpendicular to the surface with hydrogen atoms further away (i.e., hydrogen up).[5] This orientation maximizes the water dipole interaction with the image dipole created in the electrode.[5] No upright stable positions were identified in the present work or in other DFT studies of water monomers on gold surfaces.[5,53] This means that the Au−H_2O covalent interactions (i.e., Au−O and/or Au−OH interactions) dominate the behavior of the water molecule on the gold surface in the absence of an electric field.

The electrostatic interaction is studied using classical theory to better understand its interplay with the covalent energy calculated from DFT. This allows one to compare the energetic preferences of the water molecule binding geometries of hydrogen up, hydrogen down, and flat from an electrostatic point of view in the presence and absence of the field.

The total electrostatic energy of a dipole on a surface of a metal, U_{tot}, has three components: (1) the energy due to the dipole interaction with itself, i.e., with its image mandated by the "method of images" (U_{img}), (2) the energy due to the interaction of the dipole with an external applied field (U_{ext}), and (3) the often neglected[59] energy due to the polarization/depolarization of the dipole along its axis in the presence of an electrical field (U_p). A dipole subjected to an electric field in the same (opposite) direction of the dipole will be polarized (depolarized) by that field resulting in a change in the permanent dipole moment of the molecule, μ_0, by a value proportional to the applied field and polarizability constant δ.

The model developed here is based on ref 59. The self-image energy and polarizability energy were considered in ref 59 but not simultaneously with the energy due to the external field. However, closely following the analyses in ref 59 and assuming a water molecule with hydrogen up orientation as shown in Figure 5, the following expression for the total energy including the effect of the external field can be deduced:

$$U_{tot} = U_{img} + U_{ext} + U_p = -\frac{1}{2}\mu E_{img} - \frac{1}{2}\mu E_{ext} + \frac{1}{2}E_t(\mu - \mu_0) \quad (1)$$

where E_{img} is the electric field due to the dipole image, E_{ext} is the external applied field, E_t is the total electric field (E_{img} + E_{ext}), μ_0 is the dipole of the water molecule (1.86 D), and μ is the dipole after being polarized/depolarized by the total field (due to dipole image and the external field). The sign notation corresponds to the schematic in Figure 5 where E_{ext} is negative for the hydrogen down orientation.

With reference to Figure 5, the dipole in the presence of E_{img} and E_{ext} is defined as

$$\mu = \mu_0 + 4\pi\varepsilon_0\delta(E_{img} + E_{ext}) \quad (2)$$

where ε_0 is the vacuum permittivity and δ is the polarizability along the direction of the dipole which is 1.48 Å[60] (similar to cgs units). Rationalized MKS units are used throughout except for δ ($\delta_{MKS} = 4\pi\varepsilon_0\delta_{cgs}$). Polarization vanishes if the field is perpendicular to the dipole.[59] The field due to the dipole image is related to the distance of the center of the dipole from the metal surface, β, and the dipole distance, d, as shown in Figure 5. E_{img} is given by the expression below[59]

dx.doi.org/10.1021/jp408001t | J. Phys. Chem. C 2014, 118, 3459−3470

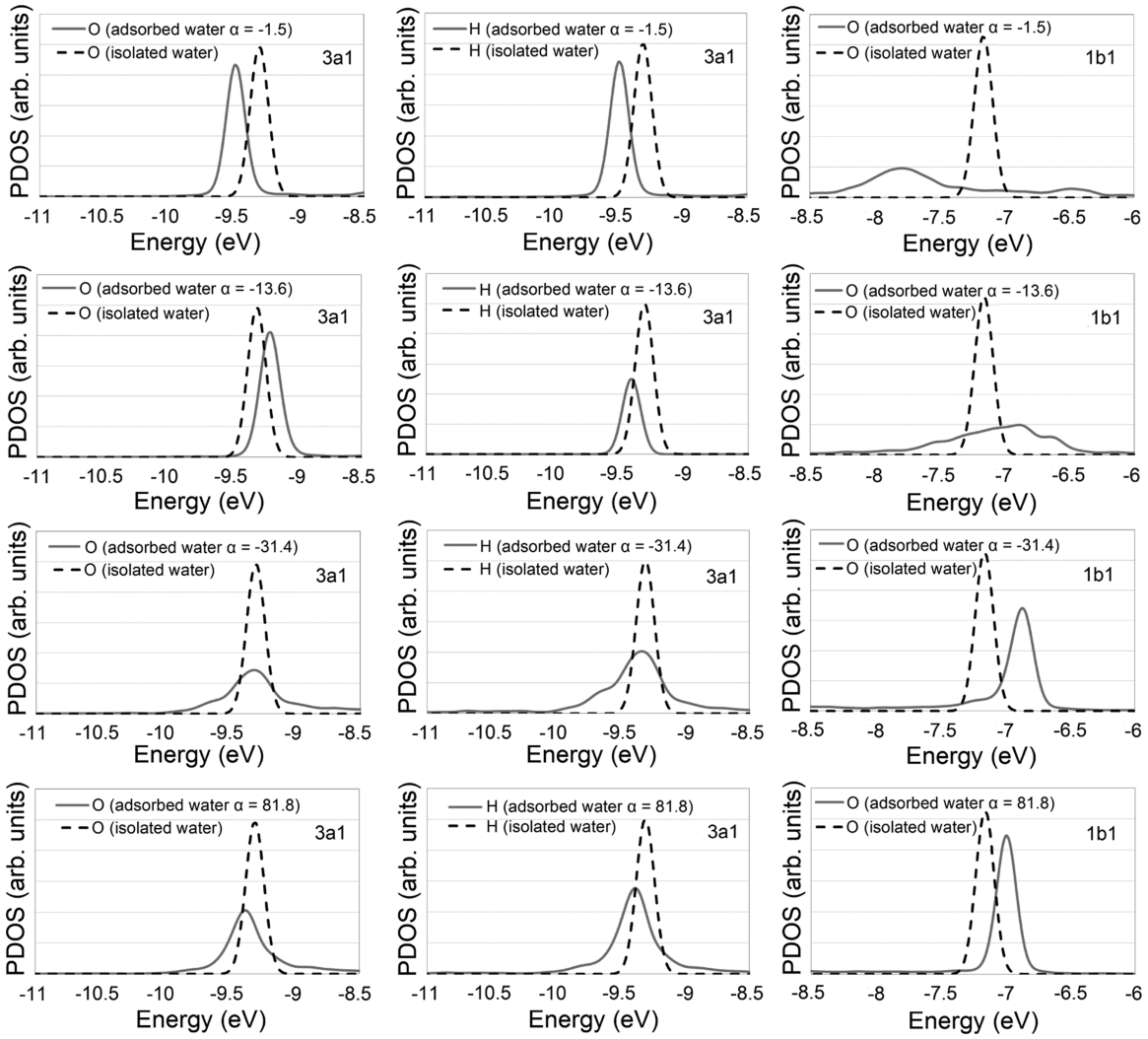

Figure 4. PDOS of water monomer at the atop position on Au(111): (left) contribution of oxygen atom to the state corresponding to the $3a_1$ orbital of the water molecule: (middle) contribution of hydrogen atoms to the state corresponding to the $3a_1$ orbital of water molecule; (right) contribution of oxygen atom to the state corresponding to the $1b_1$ orbital of water molecule (lone pair).

$$E_{\text{img}} = \frac{\mu}{16\pi\varepsilon_0\beta^3}\left[\frac{1}{1-\left(\frac{d}{2\beta}\right)^2}\right] \tag{3}$$

When eq 3 is substituted into eq 2, μ can be rewritten as

$$\mu = \mu_0 + \frac{4\pi\varepsilon_0\alpha E_{\text{ext}}}{1-\frac{\alpha}{4\beta^3\left(1-\frac{d}{2\beta}\right)^2}} \tag{4}$$

For given values of E_{ext}, β, and d, eqs 1, 3, and 4 can be used to determine the difference in the total electrostatic energy between hydrogen up and hydrogen down orientations. Applying the methods of refs 59 and 56 and substituting q by μ_0/d gives E_{img} for a flat orientation as

$$E_{\text{img}} = \frac{{\mu_0}^2}{8\pi\varepsilon_0 d^2}\left(\frac{1}{\beta-\frac{d}{2}} + \frac{2}{\sqrt{d^2+4\left(\beta-\frac{d}{2}\right)^2}}\right) \tag{5}$$

For Au(111), β and d extracted from the DFT computations are 2.9 and 0.63 Å, respectively. These values are representative values for various stable sites. A sensitivity analysis shows that the energy values are not sensitive to a variation in d and β in the range observed in the DFT results of this work. At zero external field, the hydrogen up orientation is favored over hydrogen down and flat orientations by 0.011 and 0.004 eV, respectively. The electrostatic energy together with the covalent energy is what decides the final water molecule interaction with the metal surface. The electrostatic energy is about an order of magnitude less than the lowest binding energy observed in the present work, and thus it is unlikely to play a role in deciding the water geometry. In the presence of the external field this changes significantly. The electrostatic interaction starts to play a more important role when an electric field is applied and it becomes more dominant as the magnitude of the electric field increases.

Effect of Electric Field. The electric field with a magnitude and direction varying from -5×10^9 to $+5 \times 10^9$ V/m was applied normal to the surface. The surface charge density resulting from the applied field is approximately 5% less than that calculated by Gauss' law, assuming a single infinitely extended thin sheet of surface charge density. The electric field

dx.doi.org/10.1021/jp408001t | J. Phys. Chem. C 2014, 118, 3459−3470

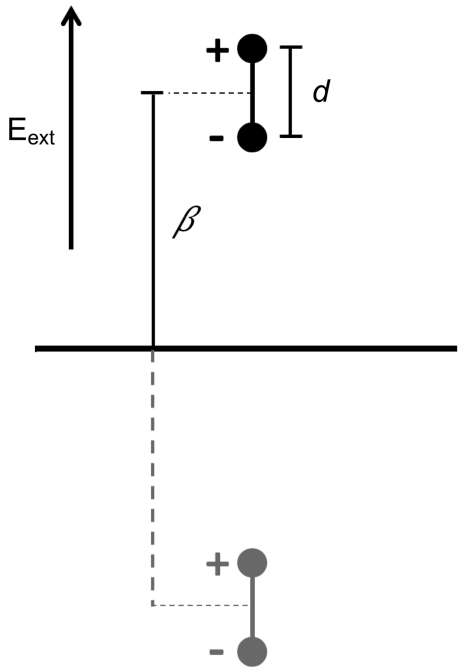

Figure 5. Schematic diagram showing a water molecule represented by a simple dipole with hydrogen up and an applied field pointing outward from the surface along the axis of the dipole.

away from the surface is defined as positive to be consistent with the definition that positive charge corresponds to the field coming out of the surface. The discussion is focused on the most stable sites, atop sites on Au(111) and Au(110), when the response of the water monomer (i.e., change in its position and geometry) to the varying electric field is considered.

The geometric response of the water monomer to the applied electric field is categorized into three responses: translation, rotation, and compression/expansion of water monomer. The schematic representations of the three types of responses are shown in Figure 6. The total translation accounts for not

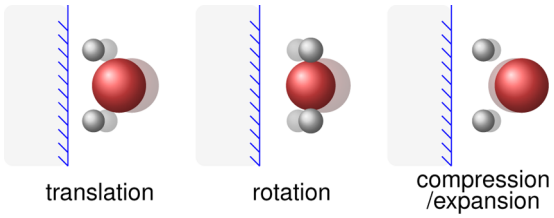

Figure 6. Three categories of the geometric change of the water molecule under the influence of an applied electric field.

only the normal component (z-direction) but also the lateral component (x- and y-directions). It should also be noted that the center of mass is used for tracing the translation of the water monomer rather than the standard way of tracing the location of the oxygen atom. The use of the center of mass decouples the rotation from the translation (e.g., there exists a change in the location of the oxygen atom when the water molecule only rotates with its center of mass fixed). Rotation only accounts for the change in bond angle as defined above because a negligible change in tangential angle is observed. Compression/expansion is described in terms of a change in the bond length and bond angle of the water monomer with respect to its equilibrium structure in the absence of the electric field.

Figure 7 shows the normal and total translation of the water monomer with respect to the applied electric field. There is a

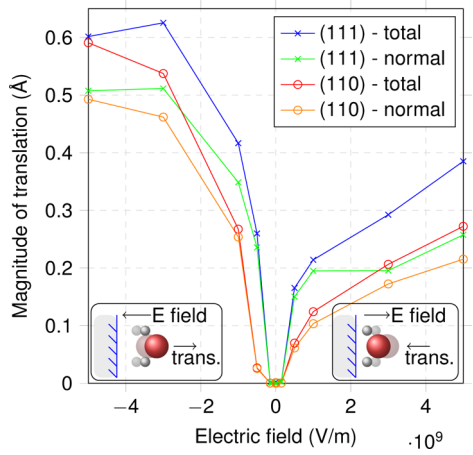

Figure 7. Total/normal translation of water monomer with respect to external electric field. A magnitude of translation is used for normal translation for comparison, but normal translation represents the water molecule moving closer to (away from) the surface when the applied electric field is positive (negative) as depicted in the right-bottom (left-bottom) illustration within.

growing difference between the normal and total translation as the applied electric field increases, indicating the emergence of lateral translation that grows with the magnitude of the electric field. It is interesting to see the lateral shift when there is only a normal component of the electric field. This result suggests that the shape of the PES deforms in response to the applied electric field and the local minima shifts in both the normal and lateral directions. In addition, the translation was nonlinear with respect to the magnitude of the applied electric field. There was virtually no translation at low electric fields up to $\sim\pm 1.5 \times 10^8$ V/m in contrast to a rapid change in position (i.e., translation) in the region when the magnitude of the electric field is between 1.5×10^8 and 1.0×10^9 V/m. The change became less sensitive to a further increase in the magnitude of the applied electric field beyond 1×10^9 V/m. The translation was also asymmetric with respect to the direction of the electric field; the translation is greater when the electric field is negative. The normal translation represents the water molecule moving toward (away from) the gold surface when the sign of the applied electric field is positive (negative). In other words, it is more difficult to move the water molecule toward the gold surface than to move it away from the surface.

The rotation of the water monomer, $\Delta\alpha$, itself does not depict much information about the orientation of the water monomer (e.g., flat, hydrogen up, hydrogen down). Because water monomer does not rotate further when it is in a complete hydrogen up or down state, it is less useful than the binding angle, α, when the initial orientation of the water monomer is not parallel to the electrode surface. Figure 8 shows the binding angle, α, of the water monomer with respect to the applied electric field. Together with the translation profile, it can be seen that the water monomer rotates to a hydrogen up (hydrogen down) orientation with its distance closer to (further away from) the surface when the electric field is positive (negative). Similar to the characteristics for translation, rotation is also found to be

dx.doi.org/10.1021/jp408001t | J. Phys. Chem. C 2014, 118, 3459−3470

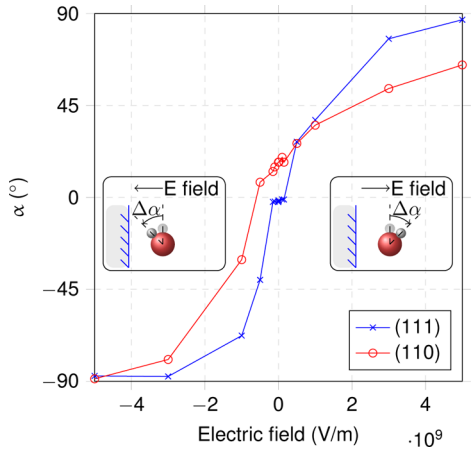

Figure 8. Binding angle of water monomer with respect to applied normal electric field.

nonlinear and asymmetric. The orientation of the water monomer becomes hydrogen up and hydrogen down with the positive and negative electric field, respectively. This agrees with the conventional belief and the unanimous conclusion from both theoretical and experimental works (refs 3, 10, 19, 27, and 30 to list a few).

In the absence of the applied field, the electrostatic energy is about an order of magnitude smaller than the total adsorption energy mainly due to the Au−O and Au−OH interactions. The rotation is the result of the applied electric field, which makes the electrostatic energy more dominant as the field magnitude is increased as shown in Figure 9. As the applied field increases,

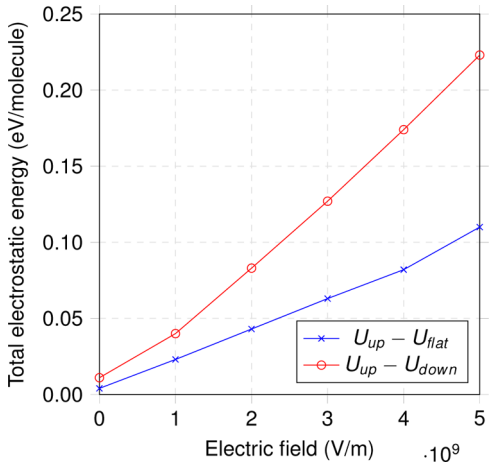

Figure 9. Total electrostatic energy difference with respect to applied normal electric field.

U_{ext}, which comes from the interaction of the water dipole with an external field, also increases. Accordingly, the electrostatic energy dominates over the covalent energy and the hydrogen up orientation becomes more favorable. As the field increases, the water molecule rotates to align itself with the field as the energy of the dipole−field interaction overcomes the covalent Au−O and Au−OH interactions.

The main conclusion is that, although the electrostatic view of the water molecule geometry favors a hydrogen up orientation in the absence of an external field, it is unlikely to find such an orientation because the covalent energy overwhelms the electrostatic energy by about an order of magnitude. In the case where the applied electric field is high enough to cause the electrostatic energy to overwhelm the covalent energy, however, the situation changes. The orientation of the water monomer is then determined by the direction of the electric field.

An interesting observation, however, is that a complete rotation (i.e., close to ±90°) is more difficult to achieve when a positive electric field is applied. The (close to) complete rotation of the water monomer was achieved at $+5.0 \times 10^9$ V/m and -3.0×10^9 V/m on Au(111) whereas it was achieved at -5.0×10^9 V/m for a negative electric field and was never achieved for a positive electric field on Au(110). This observation is quite different from the trend observed by Sánchez,[10] which reported a rather symmetric rotation of the water molecule on Ag(111) with the complete rotation achieved at a surface charge density of 15.7 μC/cm^2 (~1.77×10^{10} V/m). However, the witnessed asymmetry of this work agrees with the result of the molecular dynamics investigation of Willard et al.[61] of a pure water solution between the two metallic electrodes. They computed the capacitance of 8.39 and 5.20 μC/cm^2 on positively and negatively charged electrodes, respectively.

The rotation of the water molecule to a complete hydrogen up or down orientation is referred to as dielectric saturation.[62] On a more rigorous note, it refers to a state where the water molecule cannot translate, rotate, or compress/expand further to lower the value of the polarization density in the case of a higher electric field. The inspection of Figure 7 and 8 does not provide a full picture and it requires the structural change (i.e., change in bond angle and bond length) of the water molecule, which is attributed to the compression/expression of the monomer. There is no significant change in bond length; the maximum observed change in bond length was about 1%. The change in bond angle in the presence of the applied electric field is shown in Figure 10. No significant change in bond angle

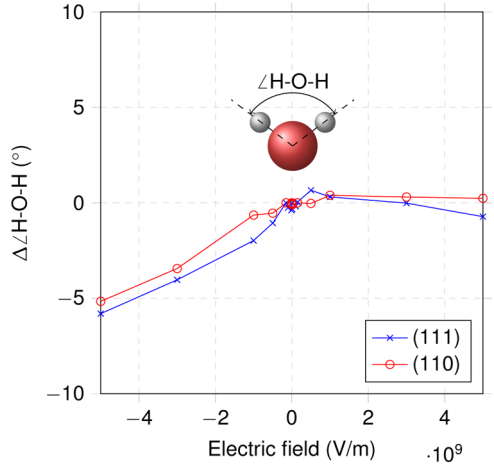

Figure 10. Change in bond angle of water monomer with respect to applied normal electric field.

in observed when a positive electric field is applied. However, there is a linear decrease in bond angle with respect to the magnitude of the electric field when a negative electric field is applied. For the electric field strengths applied in the present work, dielectric saturation was practically only achieved for the atop site of Au(111) when a negative electric field was applied (i.e., a further increase in the magnitude of the electric field

dx.doi.org/10.1021/jp408001t | J. Phys. Chem. C 2014, 118, 3459−3470

only causes a slight change in bond angle). The main features of the response of the water monomer to an electric field are the strong nonlinearity and asymmetry that is to be expected from an asymmetric molecule such as water.

Comparison of Au(111) and Au(110). As noted above, the adsorbed water monomers on Au(110) in general have a higher adsorption energy than those on Au(111). This is in line with the conclusion by Koverga et al.[13] where they found a stronger CO binding to more atomically open Au(110) over Au(111). The higher adsorption energy of water molecules on Au(110) is correlated to the less elongation of the OH bond length on Au(110) as well as the smaller rotation of the water monomer when the electric field is applied. The water molecule with stronger adsorption energy tends to respond less to the applied field, as seen in the water molecules at atop sites of Au(111) and Au(110). The difference between the interaction of water with Au(110) and Au(111) in both the absence and presence of an electric field imply that the surface morphology (i.e., structure, crystal orientation, surface packing, etc.) is an equally important factor as the chemical composition of the electrode. The $\Delta\rho$ analysis shows that the interaction of the water molecule is localized within the surface layer of atoms, which further stresses the importance of the surface conditions on the water interaction at the surface. The differences of infrared absorption and energy loss spectroscopy of water on Ag(100) and Au(111) has been attributed to the difference in morphology rather than chemical composition.[29] The spectra of water on Au(111) and Au(100) have the same trend yet the intensity differs, which further supports the important role that surface morphology plays in the interaction of water molecules on gold surfaces as observed in the present work.

CONCLUSIONS

The interface between the water monomer and gold electrode was investigated with and without an external electric field. The locations and orientations of a stable water monomer on Au(111) and Au(110) were identified and they include multiple stable sites other than the most stable atop position. The differences in the adsorption energy of all of the stable sites of Au(111) and Au(110) were both within 0.06 eV, and thus, the PES is expected to be relatively smooth. Further investigation, possibly a nudged elastic band method coupled with DFT, is necessary to make an accurate statement on the relative stability of various adsorption sites. In the presence of an external electric field, both translation and rotation were nonlinear and asymmetric with respect to the electric field. Water monomer translated and rotated more to a negative electric field than to a positive electric field. The maximum elongation of the water bond length and the maximum decrease of the water bond angle were observed to be around 1% and 5°, respectively.

The interaction between the water monomer and Au electrode with/without the electric field is explained in terms of the interplay of Au−O, Au−OH, and electrostatic interactions. In the absence of the electric field, the H_2O/Au interaction is dominated by Au−O and Au−OH interactions. The PDOS demonstrates that the Au−OH interaction plays a major role that cannot be neglected, particularly at positions other than the atop. The Au−O interaction is dominant at the atop site and the Au−OH interaction plays a bigger role at other sites. The flatter the molecule the larger the role that Au−O plays through the water $1b_1$ (lone pair) orbital and the more perpendicular the molecule the larger the role Au−OH plays through the $3a_1$ orbital. The electrostatic energy suggests that a hydrogen up orientation is energetically more favorable than a flat or a hydrogen down orientation. In the absence of the external field, the electrostatic energy is about an order of magnitude less than the covalent energy. Accordingly, the covalent interaction of Au−O and Au−OH determines the stable orientations observed: the flat at the atop site and the hydrogen down at other sites. When an electric field is applied, however, the situation changes. The contribution of the electrostatic energy associated with the interaction of the applied field with the water dipole increases as the magnitude of the electric field increases. As a result, the electrostatic energy becomes more dominant and the orientation of the water monomer is determined by the direction of the electric field.

The response of the water monomer to the electric field is related to its adsorption energy where higher (lower) adsorption energy yields a weaker (stronger) response to the field. The localized water−electrode interaction within the surface layer and the correlation between the adsorption energy and the response of the water monomer to the field indicate the importance of the surface morphology of the electrode. This could have major implications on the design of electrodes for applications such as electrochemical energy storage devices and electrolyzers. Whether such a claim could be generalized to other FCC metals or carbon based material requires further investigation.

AUTHOR INFORMATION

Corresponding Author

*A. Huzayyin: e-mail, a.huzayyin@utoronto.ca.

Notes

The authors declare no competing financial interest.

REFERENCES

(1) Baldelli, S. Probing Electric Fields at the Ionic Liquid-Electrode Interface Using Sum Frequency Generation Spectroscopy and Electrochemistry. *J. Phys. Chem. B* **2005**, *109*, 13049−13051.

(2) Osawa, M.; Tsushima, M.; Mogami, H.; Samjeske, G.; Yamakata, A. Structure ofWater at the Electrified Platinum-Water Interface: A Study by Surface-Enhanced Infrared Absorption Spectroscopy. *J. Phys. Chem. C* **2008**, *112*, 4248−4256.

(3) Stuve, E. M. Ionization of Water in Interfacial Electric fields: An Electrochemical View. *Chem. Phys. Lett.* **2012**, *519*−*520*, 1−17.

(4) Hodgson, A.; Haq, S. Water Adsorption and the Wetting of Metal Surfaces. *Phys. Rev. Lett.* **2009**, *64*, 381−451.

(5) Michaelides, A.; Ranea, V.; de Andres, P.; King, D. General Model for Water Monomer Adsorption on Close-Packed Transition and Noble Metal Surfaces. *Phys. Rev. Lett.* **2003**, *90*, 216102.

(6) Filhol, J.-S.; Neurock, M. Elucidation of the Electrochemical Activation of Water over Pd by First Principles. *Angew. Chem., Int. Ed.* **2006**, *45*, 402−406.

(7) Wilhelm, F.; Schmickler, W.; Spohr, E. Proton Transfer to Charged Platinum Electrodes. A Molecular Dynamics Trajectory Study. *J. Phys.: Condens. Matter* **2010**, *22*, 175001.

(8) Wilhelm, F.; Schmickler, W.; Nazmutdinov, R.; Spohr, E. Modeling Proton Transfer to Charged Silver Electrodes. *Electrochim. Acta* **2011**, *56*, 10632−10644.

(9) Skúlason, E.; Karlberg, G. S.; Rossmeisl, J.; Bligaard, T.; Greeley, J.; Jónsson, H.; Nørskov, J. K. Density Functional Theory Calculations for the Hydrogen Evolution Reaction in an Electrochemical Double Layer on the Pt(111) Electrode. *Phys. Chem. Chem. Phys.* **2007**, *9*, 3241−3250.

(10) Sánchez, C. G. Molecular Reorientation of Water Adsorbed on Charged Ag(111) Surfaces. *Surf. Sci.* **2003**, *527*, 1−11.

(11) Wasileski, S. A.; Koper, M. T. M.; Weaver, M. J. Metal Electrode-Chemisorbate Bonding: General Inuence of Surface Bond Polarization on Field-Dependent Binding Energetics and Vibrational Frequencies. *J. Chem. Phys.* **2001**, *115*, 8193−8203.
(12) Wasileski, S. A.; Koper, M. T. M.; Weaver, M. J. Field-Dependent Electrode-Chemisorbate Bonding: Sensitivity of Vibrational Stark Effect and Binding Energetics to Nature of Surface Coordination. *J. Am. Chem. Soc.* **2002**, *124*, 2796−2805.
(13) Koverga, A. A.; Frank, S.; Koper, M. T. Density Functional Theory Study of Electric Field Effects on CO and OH Adsorption and Co-adsorption on Gold Surfaces. *Electrochim. Acta* **2013**, *101*, 244−253.
(14) Patrito, E.; Paredes-Olivera, P. Adsorption of Hydrated Hydroxide and Hydronium Ions on Ag(111). A Quantum Mechanical Investigation. *Surf. Sci.* **2003**, *527*, 149−162.
(15) Firment, L. E.; Somorjai, G. A. Low-Energy Electron Diffraction Studies of Molecular Crystals: The Surface Structures of Vapor-Grown Ice and Naphthalene. *J. Chem. Phys.* **1975**, *63*, 1037−1038.
(16) Doering, D. L.; Madey, T. E. The Adsorption of Water on Clean and Oxygen-Dosed Ru(011). *Surf. Sci.* **1982**, *123*, 305−337.
(17) Ibach, H. Vibration Spectroscopy of Water on Stepped Gold Surfaces. *Surf. Sci.* **2010**, *604*, 377−385.
(18) Ataka, K.-i.; Osawa, M. In Situ Infrared Study of Water-Sulfate Coadsorption on Gold(111) in Sulfuric Acid Solutions. *Langmuir* **1998**, *14*, 951−959.
(19) Ataka, K.-i.; Yotsuyanagi, T.; Osawa, M. Potential-Dependent Reorientation of Water Molecules at an Electrode/Electrolyte Interface Studied by Surface-Enhanced Infrared Absorption Spectroscopy. *J. Phys. Chem.* **1996**, *100*, 10664−10672.
(20) Wandlowski, T.; Ataka, K.; Pronkin, S.; Diesing, D. Surface Enhanced Infrared Spectroscopy—Au(1 1 1−20nm)/Sulphuric Acid—New Aspects and Challenges. *Electrochim. Acta* **2004**, *49*, 1233−1247.
(21) (a) Osawa, M.; Ataka, K.-i.; Yoshii, K.; Yotsuyanagi, T. Surface-Enhanced Infrared ATR Spectroscopy for in Situ Studies of Electrode/Electrolyte Interfaces. *J. Electron Spectrosc. Relat. Phenom.* **1993**, *64*−*65*, 371−379. (b) Osawa, M.; Yoshii, K.; Ataka, K.-i.; Yotsuyanagi, T. Real-Time Monitoring of Electrochemical Dynamics by Submillisecond Time-Resolved Surface-Enhanced Infrared Attenuated-Total-Reection Spectroscopy. *Langmuir* **1994**, *10*, 640−642.
(22) Morgenstern, K.; Nieminen, J. Intermolecular Bond Length of Ice on Ag(111). *Phys. Rev. Lett.* **2002**, *88*, 066102.
(23) Morgenstern, K.; Rieder, K.-H. Formation of the Cyclic Ice Hexamer via Excitation of Vibrational Molecular Modes by the Scanning Tunneling Microscope. *J. Chem. Phys.* **2002**, *116*, 5746−5752.
(24) Mitsui, T. Water Diffusion and Clustering on Pd(111). *Science* **2002**, *297*, 1850−1852.
(25) Morgenstern, M.; Michely, T.; Comsa, G. Anisotropy in the Adsorption of H_2O at Low Coordination Sites on Pt(111). *Phys. Rev. Lett.* **1996**, *77*, 703−706.
(26) Michaelides, A. Density Functional Theory Simulations of Water−Metal Interfaces: Waltzing Waters, a Novel 2D Ice Phase, and More. *Appl. Phys. A: Mater. Sci. Process.* **2006**, *85*, 415−425.
(27) Thiel, P. A.; Madey, T. E. The Interaction of Water with Solid Surfaces: Fundamental Aspects. *Surf. Sci. Rep.* **1987**, *7*, 211−385.
(28) Carrasco, J.; Hodgson, A.; Michaelides, A. A Molecular Perspective of Water at Metal Interfaces. *Nat. Mater.* **2012**, *11*, 667−674.
(29) Ibach, H. Electron Energy Loss Spectroscopy of the Vibration Modes of Water on Ag(100) and Ag(115) Surfaces and Comparison to Au(100), Au(111) and Au(115). *Surf. Sci.* **2012**, *606*, 1534−1541.
(30) Garcia-Araez, N.; Rodriguez, P.; Navarro, V.; Bakker, H. J.; Koper, M. T. M. Structural Effects on Water Adsorption on Gold Electrodes. *J. Phys. Chem. C* **2011**, *115*, 21249−21257.
(31) Kohn, W. Nobel Lecture: Electronic Structure of Matter—Wave Functions and Density Functionals. *Rev. Mod. Phys.* **1999**, *71*, 1253−1266.
(32) Artacho, E.; Anglada, E.; Diéguez, O.; Gale, J.; García, A.; Junquera, J.; Martin, R.; Ordejón, P.; Pruneda, J.; Sánchez-Portal, D. The SIESTA Method; Developments and Applicability. *J. Phys.: Condens. Matter* **2008**, *20*, 064208.
(33) Troullier, N.; Martins, J. L. Efficient Pseudopotentials for Plane-Wave Calculations. *Phys. Rev. B* **1991**, *43*, 1993−2006.
(34) Perdew, J. P.; Burke, K.; Ernzerhof, M. Generalized Gradient Approximation Made Simple. *Phys. Rev. Lett.* **1996**, *77*, 3865−3868.
(35) (a) Feynman, R. P. Forces in Molecules. *Phys. Rev.* **1939**, *56*, 340−343. (b) Hellmann, H. *Einführung in die Quantenchemie*; Franz Deuticke: Leipzig, 1937; p 285.
(36) Ordejón, P. Linear Scaling ab initio Calculations in Nanoscale Materials with SIESTA. *Phys. Status Solidi B* **2000**, *217*, 335−356.
(37) Ramprasad, R.; Shi, N.; Tang, C. Modeling the Physics and Chemistry of Interfaces in Nanodielectrics. In *Dielectric Polymer Nanocomposites*; Nelson, J. K., Ed.; Springer US: New York, 2010; Chapter 5, pp 133−161.
(38) Ceponkus, J.; Uvdal, P.; Nelander, B. Far-Infrared Band Strengths in the Water Dimer: Experiments and Calculations. *J. Phys. Chem. A* **2008**, *112*, 3921−3926.
(39) Benedict, W. S.; Gailar, N.; Plyler, E. K. Rotation-Vibration Spectra of Deuterated Water Vapor. *J. Chem. Phys.* **1956**, *24*, 1139−1165.
(40) Darwent, B. d. *Bond Dissociation Energies in Simple Molecules*; NSRDS-NBS 31; Natl. Stand. Ref. Data Ser. (U.S., Natl. Bur. Stand.); U.S. Government Printing Office: Washington, DC, 1970.
(41) Ashcroft, N. W.; Mermin, N. D. *Solid State Physics*, 1st ed.; Holt, Rinehart and Winston: New York, 1976.
(42) Hansson, G.; Flodström, S. Photoemission Study of the Bulk and Surface Electronic Structure of Single Crystals of Gold. *Phys. Rev. B* **1978**, *18*, 1572−1585.
(43) Carrasco, J.; Klimeš, J.; Michaelides, A. The Role of van der Waals Forces in Water Adsorption on Metals. *J. Chem. Phys.* **2013**, *138*, 024708.
(44) Ren, J.; Meng, S. First-Principles Study of Water on Copper and Noble Metal (110) Surfaces. *Phys. Rev. B* **2008**, *77*, 054110.
(45) Phatak, A. A.; Delgass, W. N.; Ribeiro, F. H.; Schneider, W. F. Density Functional Theory Comparison of Water Dissociation Steps on Cu, Au, Ni, Pd, and Pt. *J. Phys. Chem. C* **2009**, *113*, 7269−7276.
(46) Kumagai, T.; Kaizu, M.; Okuyama, H.; Hatta, S.; Aruga, T.; Hamada, I.; Morikawa, Y. Water Monomer and Dimer on Cu(110) Studied Using a Scanning Tunneling Microscope. *J. Surf. Sci. Nanotechnol.* **2008**, *6*, 296−300.
(47) Ikemiya, N.; Gewirth, A. A. Initial Stages of Water Adsorption on Au Surfaces. *J. Am. Chem. Soc.* **1997**, *119*, 9919−9920.
(48) Wells, R. L.; Fort, T., Jr. Adsorption of Water on Clean Gold by Measurement of Work Function Changes. *Surf. Sci.* **1972**, *32*, 554−560.
(49) Galicia Hernández, J.; Cocoletzi, G.; Anota, E. DFT Studies of the Phenol Adsorption on Boron Nitride Sheets. *J. Mol. Model.* **2012**, *18*, 137−144.
(50) Heras, J. M.; Albano, E. V. Adsorption of Water on Gold Films. A Work Function and Thermal Desorption Mass Spectrometry Study. *Z. Phys. Chem.* **1982**, *129*, 11−20.
(51) Cicero, G.; Calzolari, A.; Corni, S.; Catellani, A. Anomalous Wetting Layer at the Au(111) Surface. *J. Phys. Chem. Lett.* **2011**, *2*, 2582−2586.
(52) Nadler, R.; Sanz, J. F. Effect of Dispersion Correction on the Au(1 1 1)-H2O Interface: A First-Principles Study. *J. Chem. Phys.* **2012**, *137*, 114709.
(53) Meng, S.; Wang, E. G.; Gao, S. Water Adsorption on Metal Surfaces: A General Picture from Density Functional Theory Studies. *Phys. Rev. B* **2004**, *69*, 195404.
(54) Kandoi, S.; Gokhale, A.; Grabow, L.; Dumesic, J.; Mavrikakis, M. Why Au and Cu Are More Selective Than Pt for Preferential Oxidation of CO at Low Temperature. *Catal. Lett.* **2004**, *93*, 93−100.
(55) Nadler, R.; Sanz, J. F. First-Principles Molecular Dynamics Simulations of the H2O/Cu(111) Interface. *J. Mol. Model.* **2011**, *18*, 2433−2442.

(56) Carrasco, J.; Michaelides, A.; Scheffler, M. Insight From First Principles into the Nature of the Bonding Between Water Molecules and 4d Metal Surfaces. *J. Chem. Phys.* **2009**, *130*, 184707.
(57) Schnur, S.; Groß, A. Properties of Metal-Water Interfaces Studied from First Principles. *New J. Phys.* **2009**, *11*, 125003.
(58) Zhao, J.; Chan, C.; Che, J. Effects of an Electric Field on a Water Bilayer on Ag(111). *Phys. Rev. B* **2007**, *75*, 085435.
(59) Maschhoff, B. L.; Cowin, J. P. Corrected Electrostatic Model for Dipoles Adsorbed ona Metal Surface. *J. Chem. Phys.* **1994**, *101*, 8138−8151.
(60) Mahoney, M. W.; Jorgensen, W. L. A Five-Site Model for Liquid Water and the Reproduction of the Density Anomaly by Rigid, Nonpolarizable Potential Functions. *J. Chem. Phys.* **2000**, *112*, 8910−8922.
(61) Willard, A. P.; Reed, S. K.; Chandler, D. Water at an Electrochemical Interface—A Simulation Study. *Faraday Discuss.* **2009**, *141*, 423−441.
(62) Taylor, C. D.; Neurock, M. Theoretical Insights into the Structure and Reactivity of the Aqueous/Metal Interface. *Curr. Opin. Solid State Mater. Sci.* **2005**, *9*, 49−65.